Supplementary Information

Computational simulation

Numerical simulation for the oxygen concentration gradients were performed using COMSOL Multiphysics (version 6.3, COMSOL Inc.). In microfluidic channels with different substrate composition, oxygen transport was governed by the general convection–diffusion equation (1–2).

$$\frac{\partial c_i}{\partial t} + \nabla \cdot J_i + u \cdot \nabla c_i = R_i \quad (1)$$

$$J_i = -D_i \nabla c_i \quad (2)$$

where c_i is the concentration of oxygen (mol·m^{-3}), D_i is the diffusion coefficient (m^2·s^{-1}), u is the velocity vector, and R_i represents the reaction term.

Since convection and chemical reactions were neglected (u = 0, R_i = 0), the equation simplifies to the transient diffusion equation (3).

$$\frac{\partial c_i}{\partial t} = \nabla \cdot \left(D_i \nabla c_i\right) \quad (3)$$

The model consisted of three layers: a PDMS layer (top), a microchannel filled with water (middle), and a substrate (bottom). The density and viscosity of the liquid phase were assumed to be the same as those of water (1000 kg m^{-3} and 0.001 Pa s, respectively). The oxygen diffusion coefficients were set to D_{water} = 1.9 × 10^{-9} m^2 s^{-1} and D_{PDMS} = 4.1 × 10^{-9} m^2 s^{-1}.[1]

The steady state between oxygen in the aqueous and PDMS phases is described by eqn (4):

$$k_1 c_{water} = k_2 c_{PDMS} \quad (4)$$

where k_1 = 1.0 × 10^{-2} m s^{-1} is the rate constant for oxygen transfer from water to PDMS, and k_2 = 1.7 × 10^{-2} m s^{-1} is the reverse rate constant.[2]

At both the top PDMS-water interface (top boundary) and the PDMS-glass substrate (bottom

boundary), no-flux boundary condition ($n \cdot \nabla c_i = 0$) was applied. Meanwhile, the oxygen flux at the PDMS–water interface (middle boundary) was modeled according to eqn (5).

$$J_{O_2} = \pm k_2 c_{PDMS} \pm k_1 c_{water} \quad (5)$$

where the sign depends on the diffusion direction.

For simplification, oxygen consumption and fluid flow in the aqueous phase were neglected, and the initial oxygen concentrations were set to $c_{PDMS} = 1.8$ mol m^{-3} [1] and $c_{water} = 0$ mol m^{-3}. The transient simulation was performed until the oxygen profile reached equilibrium, enabling visualization of the spatiotemporal diffusion of oxygen across from PDMS substrate to aqueous channel multilayer system.

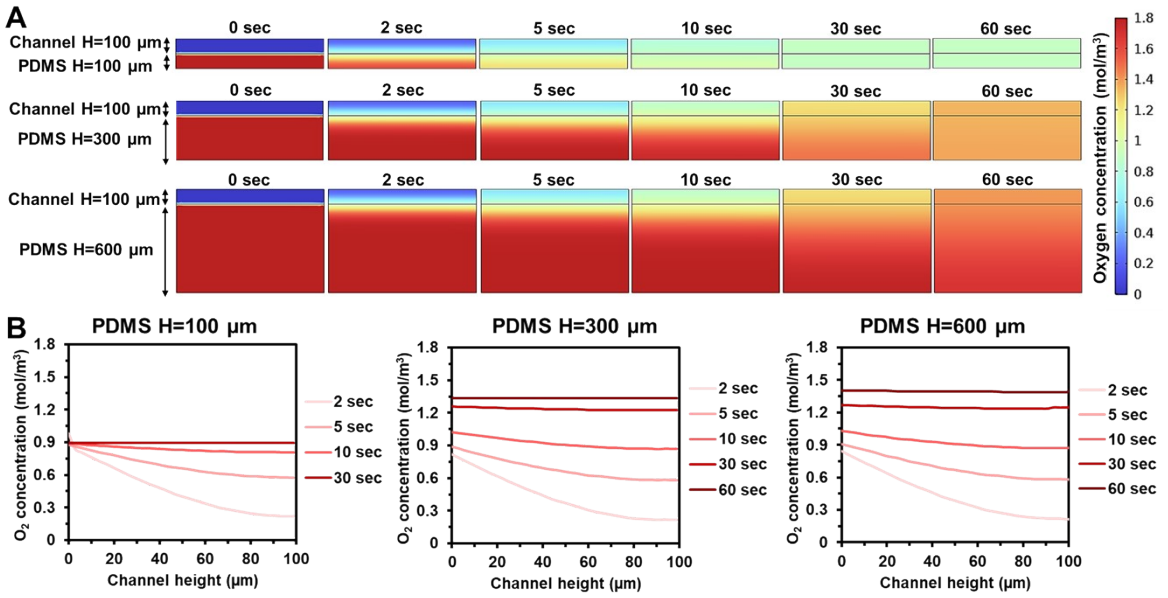

Figure S1. Numerical simulations of the time-dependent oxygen diffusion and gradients in the cul-channel. (A) Oxygen concentration profiles are visualized over time (0–60 s) for cul-channels with a fixed height of 100 μm and varying PDMS substrate thicknesses (100, 300, and 600 μm). At early time points (0–5 s), all cases exhibit steep oxygen gradients near the PDMS–water interface, indicating rapid diffusion from the PDMS bulk. In the case of a thin PDMS layer (100 μm), the oxygen concentration in the aqueous phase rapidly decreases and reache a depleted state within 10 s, suggesting an insufficient oxygen reservoir. Thicker PDMS substrates (300 and 600 μm) maintain elevated oxygen levels for prolonged periods, indicating enhanced diffusion capacity and sustained oxygen supply to the overlying aqueous region. (B)

Quantitative oxygen concentration profiles along the vertical distance from the PDMS–water interface. In thinner PDMS layers (100 μm), oxygen levels near the channel bottom decline rapidly over time, whereas thicker PDMS (≥300 μm) exhibite slower decay and higher steady-state concentrations.

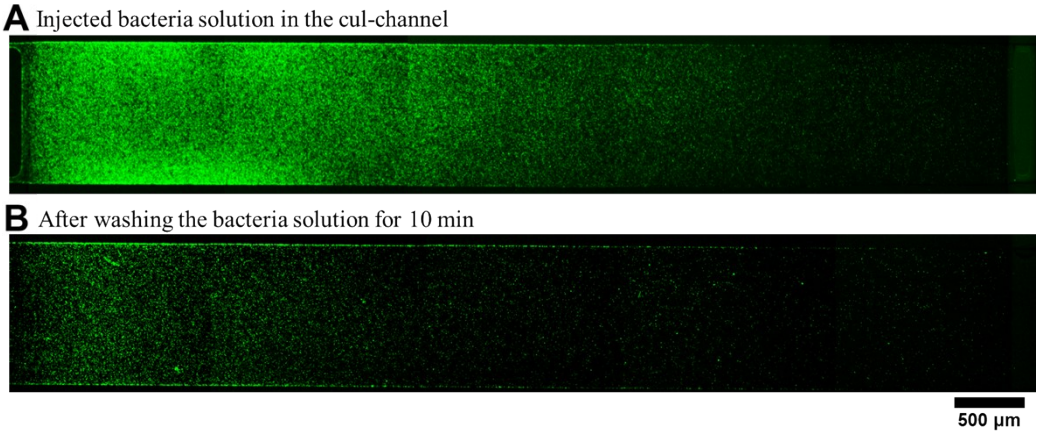

Figure S2. Fluorescence images for (A) introduced bacterial solution in the cul-channel and (B) washed bacterial solution.

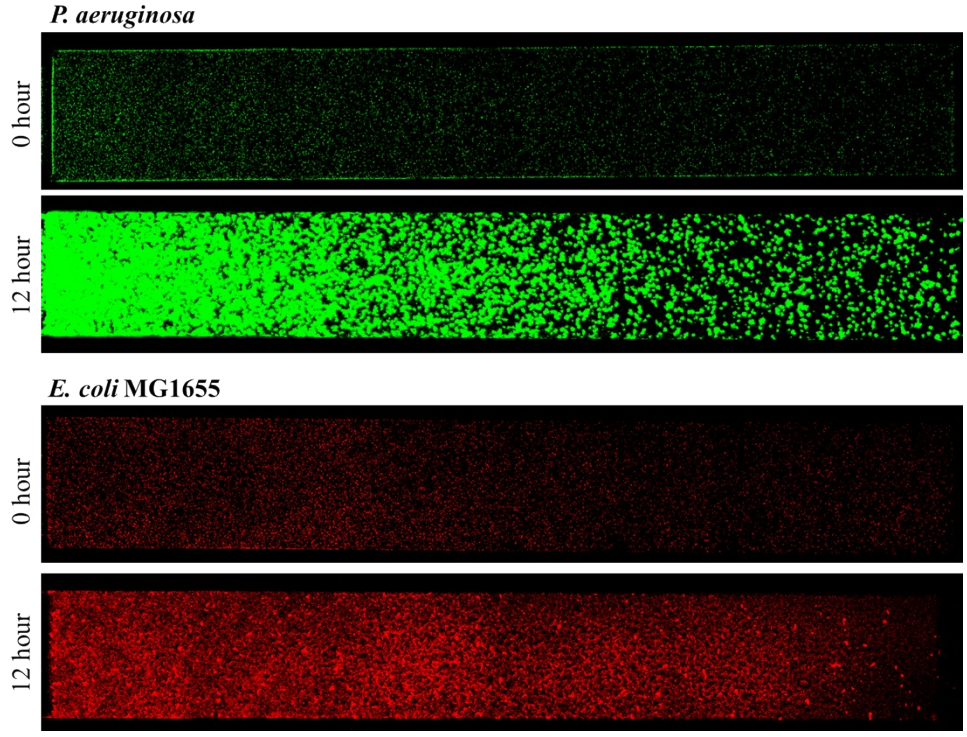

Figure S3. Biofilm formation of a single-species population density gradient. Fluorescence images showing the gradients in the population density of GFP-expressing *P. aeruginosa* and RFP-expressing *E. coli* MG1655 and the resulting biofilm structures after 12 hours.

References

1. S. Charati and S. Stern, *Macromolecules*, 1998, **31**, 5529-5535.
2. H. Shiku, T. Saito, C.-C. Wu, T. Yasukawa, M. Yokoo, H. Abe, T. Matsue and H. Yamada, *Chemistry letters*, 2006, **35**, 234-235.